Synthesis of silver-nisin nanoparticles with low cytotoxicity as antimicrobials against biofilm-forming pathogens

Zhao, Xinghong; Kuipers, Oscar P

Published in:
Colloids and Surfaces B: Biointerfaces

DOI:
10.1016/j.colsurfb.2021.111965

Publication date:
2021

Colloids and Surfaces B: Biointerfaces 206 (2021) 111965

Contents lists available at ScienceDirect

Colloids and Surfaces B: Biointerfaces

journal homepage: www.elsevier.com/locate/colsurfb

Synthesis of silver-nisin nanoparticles with low cytotoxicity as antimicrobials against biofilm-forming pathogens

Xinghong Zhao, Oscar P. Kuipers *

Department of Molecular Genetics, Groningen Biomolecular Sciences and Biotechnology Institute, University of Groningen, Groningen, 9747 AG, the Netherlands

ARTICLE INFO

Keywords:
Antimicrobial activity
Antibiofilm activity
Nanoparticle
Silver
Nisin

ABSTRACT

Wound infection is a serious threat to patients, in particular those with septic wound infections, which result in high mortality rates. Moreover, the treatment of wound infections with antimicrobial-resistant and/or biofilm-forming pathogens can be challenging. Nisin, a potent antimicrobial against Gram-positive bacterial pathogens, has been used in the food industry as a preservative for decades. Silver has been approved by the FDA as a topical antimicrobial. Here, we show that silver-nisin nanoparticles (Ag-nisin NP), with an average diameter of 60 nm, can be quickly synthesized with the assistance of a simple microwave. Ag-nisin NP act as bactericidal antibiotics against the tested pathogens. In contrast, resistance was observed in *S. aureus* and *A. baumannii* that were treated with silver nitrate alone. In addition, Ag-nisin NP showed potent antibiofilm activity against *S. aureus*, *P. aeruginosa*, *A. baumannii*, *K. pneumoniae*, and *E. coli*, which are pathogens occurring in wound infections. Notably, the synthesized Ag-nisin NP showed lower cytotoxicity than silver nitrate to human cells. This formulation provides an alternative and safe measurement for biofilm-infected wound control.

1. Introduction

The skin plays a critical role in keeping microorganisms away from the underlying tissues of the human body. Wound infection caused by mechanical disruption of the skin or by burn is a serious threat to patients [1]. Particularly, septic wound infections can result in high mortality rates [2]. Previous studies demonstrated that *Staphylococcus aureus*, *Pseudomonas aeruginosa*, *Acinetobacter baumannii*, *Klebsiella pneumoniae*, and *Escherichia coli* are major contributors to wound infections [1–6]. Moreover, antimicrobial-resistant pathogens, including multi-drug resistant *P. aeruginosa* (MDR PA), *A. baumannii* (MDR AB) and methicillin-resistant *S. aureus* (MRSA), are playing an important role in the high morbidity and mortality rate of wound infections [4]. Even more seriously, these major contributors (*S. aureus*, *P. aeruginosa*, *A. baumannii*, *K. pneumoniae*, and *E. coli*) usually form biofilms in the infected wound, and these biofilms make wound infections more difficult to treat [6]. Therefore, new alternatives are required to therapeutic treat wound infections.

Nanotechnology-based antimicrobials, which can penetrate biofilms and kill pathogens including multidrug-resistant strains, have been proposed as a promising source of antimicrobial agents [7]. Silver-based nanocomposites showed potent antimicrobial activity against planktonic pathogens as well as biofilms of pathogens [8]. Moreover, they have been shown to exert strong synergistic effects with certain antibiotics [9–11]. Silver is a widely used material for producing metal-based nanocomposites, and it is currently approved by the U.S. Food and Drug Administration (FDA) as a topical antimicrobial [12]. Nisin is a 34 amino acid post-translationally modified natural antimicrobial peptide produced by various *Lactococcus lactis* strains (Fig. 1), which has been approved and used in the food industry for decades all over the world [13,14]. Nisin exerts its bactericidal activity against Gram-positive bacteria by binding to cell wall synthesis precursor lipid II and forming pores on the cellular membranes [15–18]. Recently, the antimicrobial effects of nisin against mastitis, respiratory-, gastrointestinal- and skin infections have been investigated, and the results showed that nisin had potent antimicrobial effect against Gram-positive caused infections [19]. Therefore, silver- and nisin-based nanocomposites may show enhanced antimicrobial activity against both planktonic pathogens and pathogen biofilms in wound infections.

In this study, we introduce a simple, ultrafast and quality-stable method to construct Ag-nisin nanoparticles by employing a strategy of microwave-assisted molecular self-assembly. Under the selected conditions, Ag-nisin NP with an average diameter of 60 nm was obtained. Moreover, Ag-nisin NP showed lower cytotoxicity (half-cell toxicity)

* Corresponding author.
E-mail address: o.p.kuipers@rug.nl (O.P. Kuipers).

https://doi.org/10.1016/j.colsurfb.2021.111965
Received 18 March 2021; Received in revised form 2 June 2021; Accepted 1 July 2021
Available online 3 July 2021

than Silver nitrate to human cells, while nisin alone is known to have very low cytotoxicity too [20,21]. Notably, the synthesized Ag-nisin NP showed potent antimicrobial activity and antibiofilm activity against *S. aureus*, *P. aeruginosa*, *A. baumannii*, *K. pneumoniae*, and *E. coli*, which are pathogens responsible for wound infections. This work provides an alternative measurement for biofilm-infected wound control.

2. Results

2.1. Synthesis and characterization of Ag-nisin NP

The synthesis of Ag-nisin NP was performed with different concentrations of nisin and different microwave irradiation times, and the size of the products was determined by dynamic light scattering (DLS). Ag-nisin NP was obtained with the smallest average size under the condition of adding 4 mL of 680 mg/L silver nitrate solution to 95 mL of nisin at a concentration of 210 mg/L and microwave irradiation for 15 s at 700 W (Supplementary Figs. S1–S3). The yield of Ag-nisin NP was 3.4 mg per reaction under the optimized conditions. A scanning electron microscope (SEM) assay was used to investigate the morphology of Ag-nisin NP, and the results show that Ag-nisin NP with an irregular morphology was obtained (Fig. 2a). In addition, a transmission electron microscopy (TEM) was used to get a higher resolution morphological insight in Ag-nisin NP (Fig. 2a, right top). The size distribution of synthesized Ag-nisin NP, by counting 300 particles of SEM, is shown in Fig. 2b, and the results show that Ag-nisin NP with an average size of 60 ± 19 nm were obtained. However, the zeta-average size of the synthesized Ag-nisin NP measured by DLS, 139 nm (diameter; Supplementary Figs. S2 and S4), was 79 nm larger than the observed in the SEM, indicating the formation of a nisin coating around the Ag-nisin NP. Subsequently, X-ray diffraction (XRD) was used to investigate the phase of the Ag-nisin NP. As shown in Fig. 2c, the diffraction features appearing at 32.3°, 46.2°, 67.5° and 76.7° are corresponding to the (111), (200), (220) and (311) planes of the cubic phase of Ag, respectively [22,23]. These results indicate that silver crystals had been formed in the Ag-nisin NP. Furthermore, to verify whether the nanoparticle (Ag-nisin NP) was formed by nisin and a silver crystal, an attenuated total reflection infrared (ATR-FTIR) assay was performed. The characteristic peaks of nisin at 1658.45 and 1527.32 are corresponding to a C═O stretching of amide I and N—H bending of amide II, respectively (Fig. 2d) [24–26]. The same peaks were also observed for the Ag-nisin NP (Fig. 2d). In addition, a zeta potential assay revealed that the synthesized Ag-nisin NP has a positive potential of +23.5 ± 1.1, which is consistent with previously reported Ag-cationic peptide NP [27–29]. These results confirmed that the synthesized Ag-nisin NP consists of silver crystal and nisin. To measure the Ag-nisin NP contains how much silver crystal and nisin, the amount of nisin in the solutions (before the synthesis and after the centrifugation) was measured by high-performance liquid chromatography (HPLC). The amount of nisin decreased by 2.26 mg after the reaction, indicating that the yield Ag-nisin NP (3.4 mg) contains 2.26 mg nisin and 1.14 mg silver crystal.

2.2. Ag-nisin NP exerts potent antimicrobial activity against the tested biofilm-forming pathogens

To determine the antimicrobial activity of Ag-nisin NP, a MIC assay was performed. Silver nitrate and nisin were used as controls. Nisin showed potent antimicrobial activity against *S. aureus* (LMG15975, MRSA), which is a Gram-positive bacterium (Table 1). However, nisin showed very weak antimicrobial activity against most of the tested Gram-negative bacteria pathogens (Table 1). These results are consistent with previous studies [30–32]. Silver nitrate showed potent antimicrobial activity against all of the tested strains (Table 1). Moreover, it was shown to have a better antimicrobial activity against Gram-negative bacteria than against Gram-positive bacteria (Table 1). Ag-nisin NP showed potent antimicrobial activity against all of the tested pathogens, and it showed better antimicrobial activity against all tested pathogens than Silver nitrate (Table 1). In addition, Ag-nisin NP showed much better antimicrobial activity against the Gram-negative bacteria tested than nisin alone (Table 1).

2.3. Time-dependent killing of planktonic pathogens by Ag-nisin NP

Measuring the time-dependence of antibiotic action is commonly used to establish whether a compound is bacteriostatic or bactericidal [33,34]. In this study, we monitored the killing kinetics of *A. baumannii*, *P. aeruginosa*, *E. coli*, *K. pneumoniae* and *S. aureus* cells exposed to the synthesized Ag-nisin NP, silver nitrate or nisin. Due to its pore-formation ability in the target cell membrane, together with cell wall biosynthesis inhibition by lipid II binding, nisin is well known as a bactericidal antibiotic [15]. The time-dependent killing results show that nisin killed all of the *A. baumannii*, *E. coli* and *S. aureus* in 2 h (Fig. 3a, c and e). Moreover, nisin killed most of the *P. aeruginosa* and *K. pneumoniae* in 8 h (Fig. 3b and d). However, nisin did not completely kill *P. aeruginosa* and *K. pneumoniae* at 24 h after treatment, and both of the pathogens were grown to an OD_{600} of around 6 at 72 h after treatment. These results indicate that *P. aeruginosa* and *K. pneumoniae* are resistant against nisin. Silver nitrate showed a quick killing capacity against *E. coli*, *P. aeruginosa* and *K. pneumoniae*, killing all pathogens in 2 h (Fig. 3b–d). Although silver nitrate killed most of *A. baumannii* in 2 h, the pathogen got resistant after 8 h treatment and reached an OD_{600} of 4 after 24 h treatment (Fig. 3a). Silver nitrate showed bacteriostatic activity against *S. aureus* in 8 h after treatment, but the pathogen grew to an OD_{600} of 5 after 72 h treatment (Fig. 3a). Ag-nisin NP showed fast kill kinetics against all of the tested pathogens, which killed all of the *E. coli*, *K. pneumoniae* and *S. aureus* in 1 h after treatment (Fig. 3c–e), killed all of the *A. baumannii* in 2 h after treatment (Fig. 3a) and killed all of the *P. aeruginosa* in 4 h after treatment (Fig. 3b). These results indicate that Ag-nisin NP is the best candidate to treat a mixed wound infection among the three formulations.

2.4. Ag-nisin NP shows potent antibiofilm activity

An XTT assay was used to measure the antibiofilm activity of antimicrobial agents in previous studies [35–37]. In this study, we also used the XTT assay to investigate the antibiofilm activity of Ag-nisin NP. Nisin

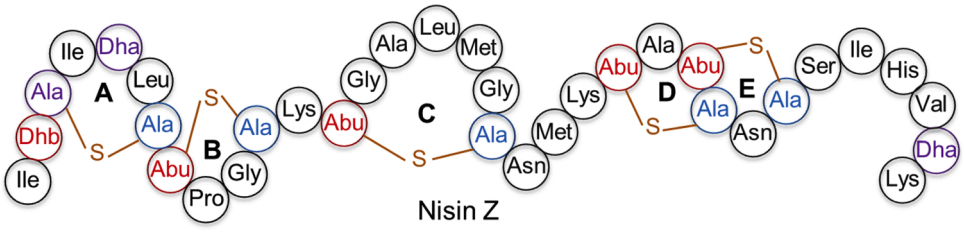

Fig. 1. Structure of the lanthipeptide nisin Z. Nisin Z is a 34 amino acids lantibiotic, which contains five (methyl)lanthionine rings. Dha: dehydroalanine, Dhb: dehydrobutyrine, Abu: aminobutyric acid.

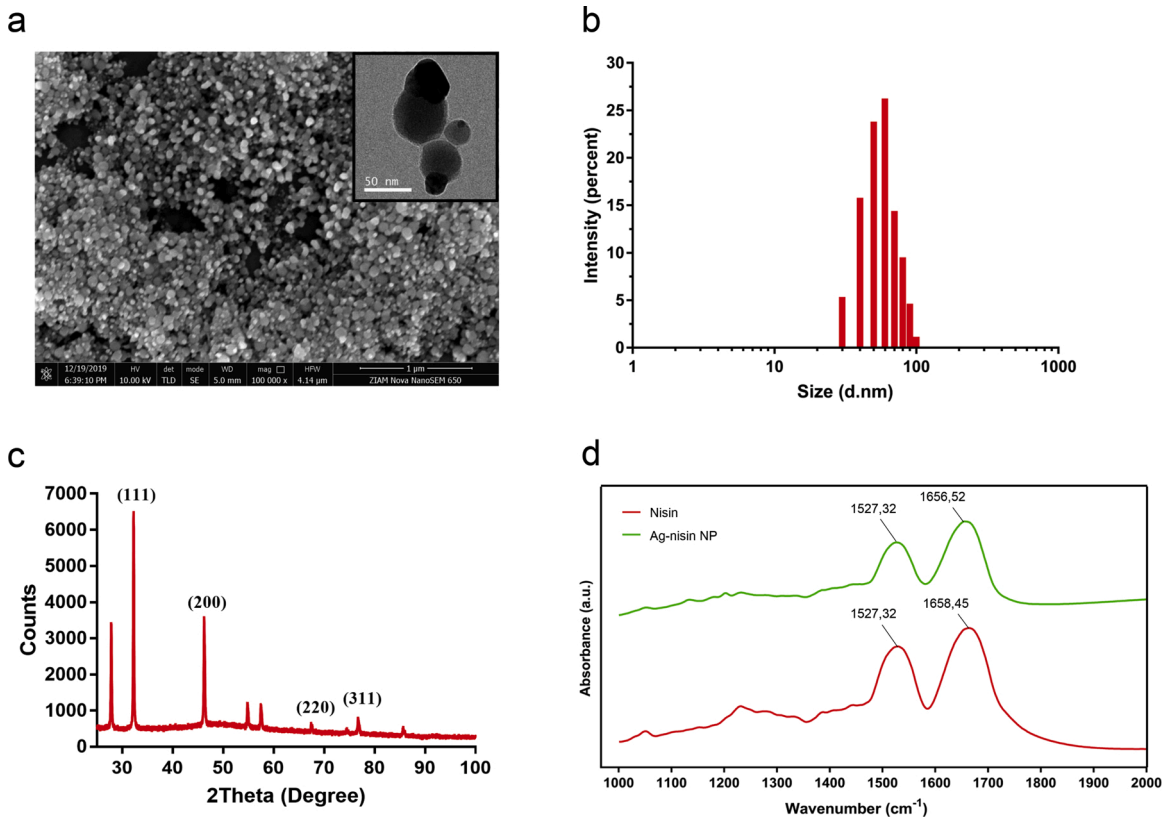

Fig. 2. Characterization of Ag-nisin NP. a, SEM of Ag-nisin NP, and TEM of Ag-nisin NP (right top); **b**, size distribution of synthesized Ag-nisin NP by counting 300 particles of SEM result (average size 60 nm); **c**, XRD of Ag-nisin NP; **d**, FTIR of Ag-nisin NP and nisin.

Table 1
Antimicrobial activity of Ag-nisin NP against pathogenic microorganisms.

Organism and genotype	MIC (mg/L)		
	Nisin	Silver nitrate	Ag-nisin NP
A. baumannii LMG01041	16	2	1
P. aeruginosa LMG 6395	128	4	2
E. coli LMG8223	64	4	2
K. pneumoniae LMG20218	128	8	4
S. aureus LMG15975 (MRSA)	4	16	4

The MIC was determined by broth microdilution. MRSA, methicillin-resistant *S. aureus*.

is an antibiotic that has established antibiofilm activity against Gram-positive bacteria [21,38,39]. Here, the results show that nisin has potent antibiofilm activity against *S. aureus* (Fig. 4a). In addition, nisin showed antibiofilm activity against *A. baumannii* (Fig. 4b). Ag-nisin NP showed potent antibiofilm activity against these tested pathogens (Fig. 4c). After 4 h of treatment, the viability of bacteria in a biofilm was only 26.8 % for *A. baumannii* and 8.4 % for *S. aureus* under a 2 × MIC treatment (Fig. 4c). In addition, under a 2 × MIC treatment, Ag-nisin NP killed 88.3 % of *P. aeruginosa*, 82.5 % of *E. coli* and 73.6 % of *K. pneumoniae* in their biofilms, respectively (Fig. 4c). Silver nitrate alone showed antibiofilm activity against the tested Gram-negative pathogens (Fig. 4d), but its showed lower antibiofilm activity than Ag-nisin NP. Moreover, silver nitrate showed insufficient antibiofilm activity against *S. aureus* (Fig. 4d). These results demonstrate that Ag-nisin NP is a good candidate for combating with biofilm infection of wound.

2.5. Ag-nisin NP showed lower cytotoxicity than silver nitrate to human cells

To assess the safety of Ag-nisin NP to human beings in an initial test, the cytotoxicity of antimicrobials to human skin fibroblasts (Hs 44.Fs, ATCC ® CRL7024™) and a human kidney epithelium cell line (HEK) was evaluated by an XTT assay. Human cells were incubated in the presence of different concentrations of antimicrobials. After 24 h incubation, the cell viability was determined by using a XTT kit. Under the experimental conditions used, human cells were unaffected by the presence of nisin at 128 μg/mL (Fig. 5c). Silver nitrate showed potent cytotoxicity to Hs 44. Fs and HEK, with a half-cell toxicity (CC_{50}) of 5.69 ± 0.17 and 3.81 ± 0.40, respectively (Fig. 5a and d), which is around most of its MIC values against pathogens (Table 1). In contrast, Ag-nisin NP did not show cytotoxicity to Hs 44.Fs and HEK at concentrations of 8 × MIC value against *A. baumannii*, 4 × MIC against *P. aeruginosa* and *E. coli*, and 2 × MIC against *K. pneumoniae* and *S. aureus* (Fig. 5b and d, Table 1). These results indicate that Ag-nisin NP is a highly efficient and low toxicity antimicrobial agent.

3. Discussion

Here we show a simple, ultrafast, and quality-stable method for Ag-nisin NP synthesis. The synthesized Ag-nisin NP showed potent antimicrobial and antibiofilm activity against *A. baumannii*, *P. aeruginosa*, *E. coli*, *K. pneumoniae* and *S. aureus*, which are common pathogens of wound infections.

Various methods have been used to construct silver nanocomposites, including chemical, physical and biological methods [40]. Microwave-assisted synthesis of silver nanocomposites has many advantages, such as smaller size, narrower size distributions, shorter reaction times, reduced energy consumption, and better product yields, than with other common methods [41,42]. In this study,

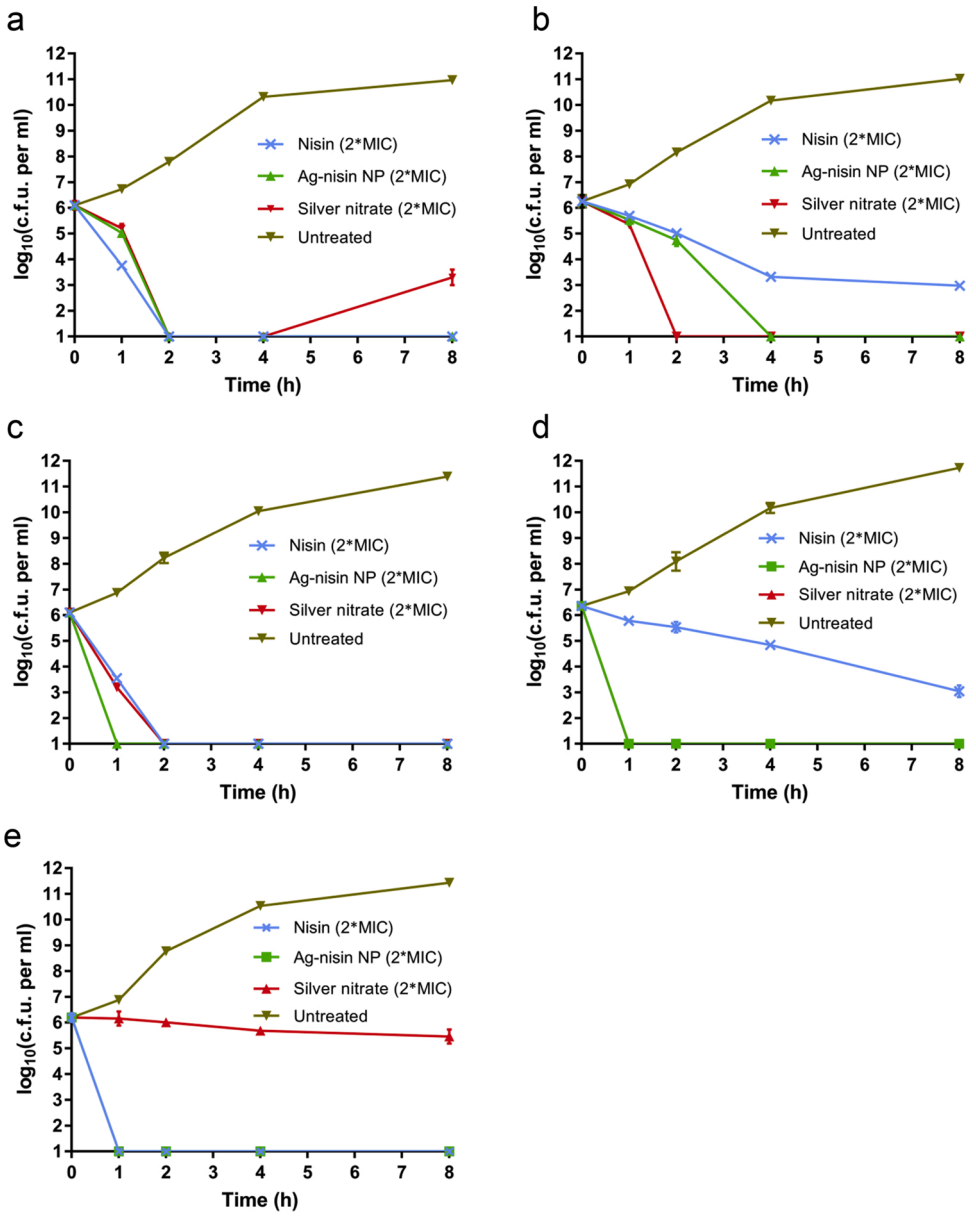

Fig. 3. Time-dependent killing of pathogens by Ag-nisin NP. Pathogens were challenged with antimicrobials (2 × MIC). **a**, *A. baumannii* (LMG01041); **b**, *P. aeruginosa* (LMG 6395); **c**, *E. coli* (LMG8223); **d**, *K. pneumoniae* (LMG20218); **e**, *S. aureus* (LMG15975, MRSA). Data are representative of three independent experiments ± s.d.

microwave-assisted synthesis of Ag-nisin NP was performed. The results showed Ag-nisin NP with an average size of 60 nm (diameter) were obtained, and it only needed 15 s to obtain this narrow size distribution of Ag-nisin NP. In contrast, previous studies showed that nisin-silver nanoparticles can be synthesized by incubation of silver nitrate and nisin at room temperature for 24 h [43], and the synthesized nisin-silver nanoparticles showed a 233 nm (diameter) average size [43], which is known to lack antibiofilm activity [7]. These results demonstrate that microwave-assisted synthesis of Ag-antimicrobial peptide nanocomposites is a much more effective approach.

Most of clinical wound infections are mixed Gram-negative and Gram-positive pathogens infections [1–6]. Nisin is a very stable molecule thanks to the lanthionine rings, but it has only potent antimicrobial activity against Gram-positive bacterial pathogens [30,31], which has limited the application of nisin as an alternative control for wound infection. Silver has a potent bactericidal effect against both Gram-positive and Gram-negative pathogens [12,44], but it's difficult to balance antimicrobial activity with cytotoxicity. In this study, the synthesized Ag-nisin NP showed comparable antimicrobial activity against both Gram-positive and Gram-negative pathogens as silver nitrate. Notably, Ag-nisin NP showed lower cytotoxicity against mammalian cells than silver nitrate alone. In contrast, the antimicrobial peptide LL37 coated LL37@AgNP decreased the antimicrobial activity of silver nitrate against Gram-negative bacterial pathogens tested [29]. These results indicate that the lanthionine-stabilized antimicrobial peptide nisin (Fig. 1) is more suitable to be used to synthesize silver nanocomposites than linear antimicrobials. The stronger antimicrobial activity, higher stability and lower cytotoxicity make Ag-nisin NP an attractive option to control wound infections.

Many of the isolates of clinical wound infections are biofilm producing strains [6]. In this study, the synthesized Ag-nisin NP showed a broad-spectrum of antibiofilm activity against both Gram-positive and Gram-negative pathogens (Fig. 5). These results are consistent with previous studies, which showed that silver nanoparticles have

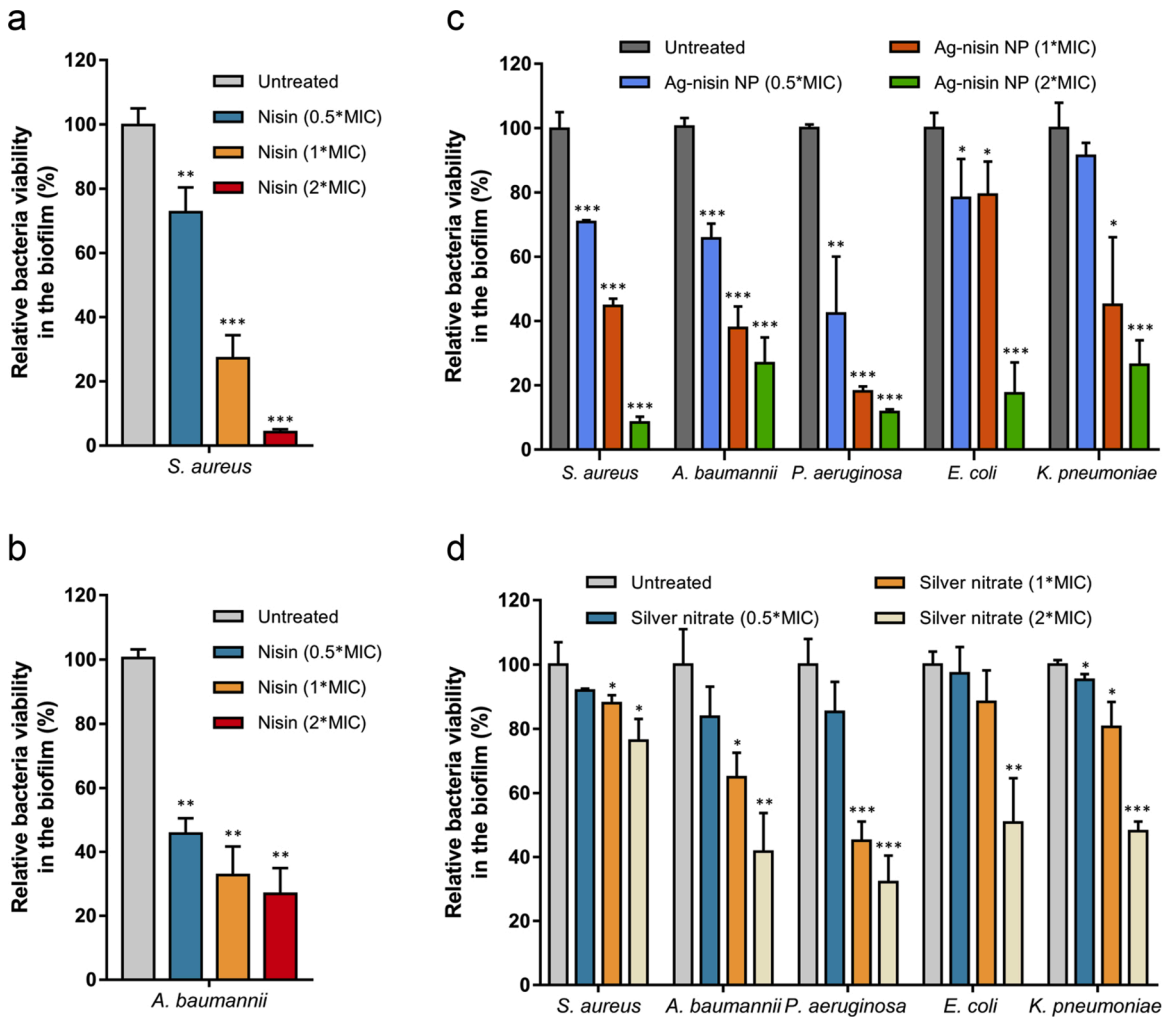

Fig. 4. Anti-biofilm activity of Ag-nisin NP. Controls were growth in Mueller-Hinton broth and without any antimicrobial treatment (Untreated). After treatment with antimicrobials for 4 h, the bacteria viability in biofilms were measure by a commercial XTT kit. **a**, Anti-biofilm activity of different concentrations of nisin against *S. aureus* (LMG15975, MRSA), nisin is an antibiotic that are known to have anti-biofilm activity; **b**, Anti-biofilm activity of different concentrations of nisin against *A. baumannii* (LMG01041); **c**, Anti-biofilm activity of different concentrations of Ag-nisin NP against *S. aureus* (LMG15975, MRSA), *A. baumannii* (LMG01041), *P. aeruginosa* (LMG 6395), *E. coli* (LMG8223) and *K. pneumoniae* (LMG20218) biofilms, respectively; **d**, Anti-biofilm activity of different concentrations of silver nitrate against *S. aureus* (LMG15975, MRSA), *A. baumannii* (LMG01041), *P. aeruginosa* (LMG 6395), *E. coli* (LMG8223) and *K. pneumoniae* (LMG20218) biofilms, respectively. Values are means ± SD (n = 3). Data are representative of three independent experiments; the statistical significance of differences was performed by Pearson r2, ns: $p > 0.05$, *$p < 0.05$, **$p < 0.01$, and ***$p < 0.001$ vs. untreated cells.

antibiofilm activity [29,45–47]. In addition, silver nanocomposites show strong synergistic effects with antibiotics [9–11]. It could be also a good strategy to use Ag-nisin NP with other antibiotics for wound infection control.

In conclusion, a microwave-assistant ultra-fast method was performed to synthesize highly effective and safe Ag-nisin NP. The synthesized Ag-nisin NP showed potent antimicrobial and antibiofilm activities against both Gram-negative and Gram-positive bacterial pathogens, which is 2–4 times better than clinically used ionic silver. Notably, the synthesized Ag-nisin NP showed lower cytotoxicity than clinically used ionic silver against a human cells. These results indicate that Ag-nisin NP offer good application possibilities to treat wound infections.

4. Materials and methods

4.1. Assembly of silver-nisin nanocomposites

Nisin (99 % purity, Handary S.A., Belgium) was dissolved in water (with an electronic resistance of 18.2 MΩ*cm, MQ) to concentrations of 420, 210 and 105 mg/L, respectively. Then 4 mL of 680 mg/L silver nitrate (Sigma) was dropped into 95 mL of nisin solution at room temperature. Under microwave irradiation at power intensity of 700 W, the reaction of the mixture was carried out for 15, 30 and 60 S, respectively. After centrifugation at 10,000 × g for 15 min, the product was washed with MQ water three times.

4.2. Characterization of Ag-nisin NP

The hydrodynamic size of Ag-nisin NP was determined by Dynamic light scattering (DLS, Malvern Panalytical), using 1.0 cm pathlength disposable cuvettes. The zeta potential of Ag-nisin NP was determined by a Malvern Zetasizer (Malvern Panalytical), using disposable 0.5 ml folded capillary cells. SEM images were recorded in vacuum on a ZIAM Nova NanoSEM 650 with an acceleration voltage of 10 kV. For TEM measurements, samples were prepared by delivering ~5 μl of solution to carbon-coated copper grids and dried in a vacuum system. The morphologies were obtained under a Philips CM120 Microscope coupled to a 4k CCD camera using an acceleration voltage of 120 kV. X-ray diffraction (XRD) patterns of Ag-nisin NP were recorded using a Bruker D8

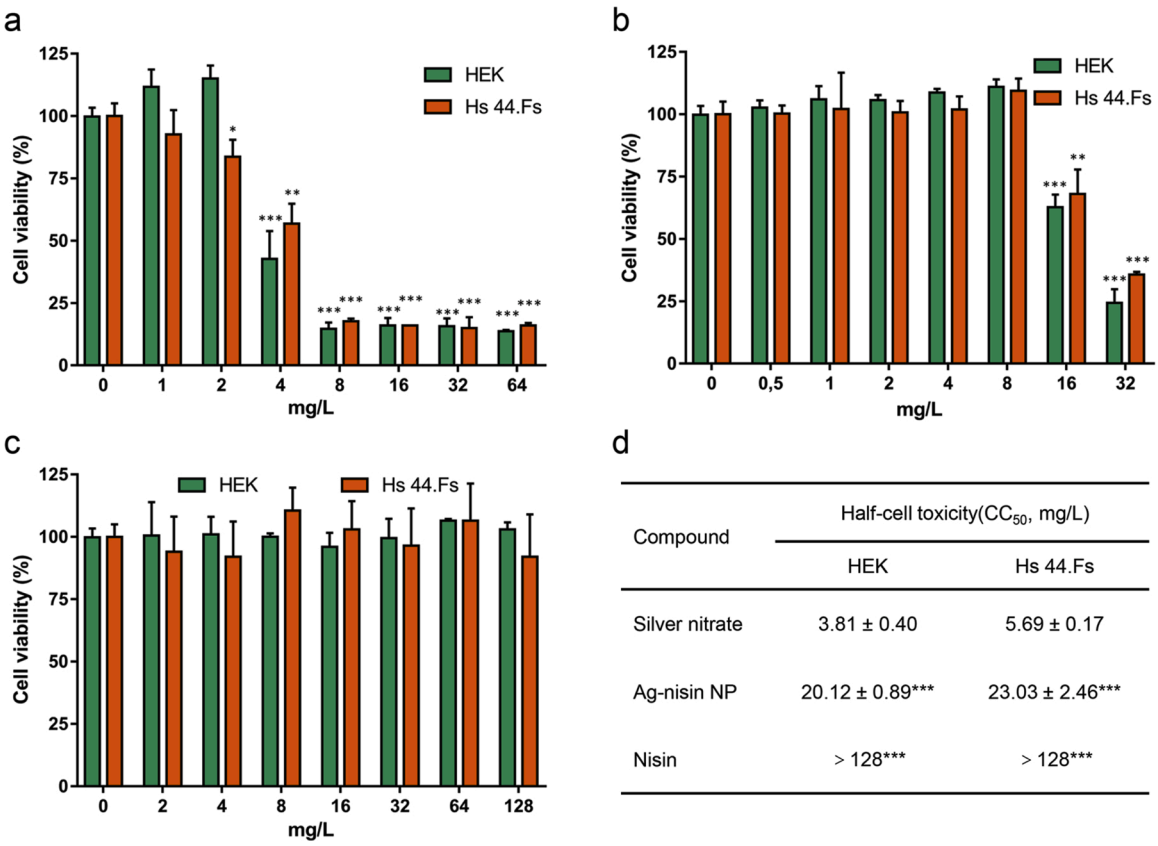

Compound	Half-cell toxicity(CC_{50}, mg/L)	
	HEK	Hs 44.Fs
Silver nitrate	3.81 ± 0.40	5.69 ± 0.17
Ag-nisin NP	20.12 ± 0.89***	23.03 ± 2.46***
Nisin	> 128***	> 128***

Fig. 5. Percentage of cell viability of human cells after 24 h treatment of different concentrations of nisin, Ag-nisin NP and Silver nitrate, respectively. a, Silver nitrate; **b**, Ag-nisin NP; **c**, Nisin. **a**, **b** and **c**, Data are representative of three independent experiments; the statistical significance of differences was performed by Pearson r2, ns: $p > 0.05$, *$p < 0.05$, **$p < 0.01$, and ***$p < 0.001$ vs. untreated cells. **d**, The 50 % cell toxicity of compound to human cells, Data are representative of three independent experiments; the statistical significance of differences was performed by Pearson r2, ns: $p > 0.05$, *$p < 0.05$, **$p < 0.01$, and ***$p < 0.001$ vs. silver nitrate treated cells.

Advance X-ray diffractometer with a Cu Kα source (λ =1.54 Å) and a Lynxeye detector. The attenuated total reflection infrared spectrometry (ATR-FTIR) of Ag-nisin was performed after mixing with potassium bromide (1:100) in an agilent cary 600 FTIR spectrometer (Agilent Technologies, USA) for the analysis of functional groups.

4.3. Minimum inhibitory concentration (MIC)

MIC values were determined by broth micro-dilution according to the standard guidelines [48], and *A. baumannii* (LMG01041), *P. aeruginosa* (LMG 6395), *E. coli* (LMG8223), *K. pneumoniae* (LMG20218) and *S. aureus* (LMG15975, MRSA)) were used as indicator strains. Briefly, the test medium was cation-adjusted Mueller-Hinton broth (MHB). Cell concentration was adjusted to approximately 5×10^5 cells per ml. After 24 h of incubation at 37 °C, the MIC was defined as the lowest concentration of antibiotic with no visible growth. Experiments were performed with biological replicates.

4.4. Planktonic time-dependent killing assay

This assay was performed according to a previously described procedure [34]. An overnight culture of cells (*A. baumannii* (LMG01041), *P. aeruginosa* (LMG 6395), *E. coli* (LMG8223), *K. pneumoniae* (LMG20218) and *S. aureus* (LMG15975, MRSA)) was diluted 50-fold in MHB and incubated at 37 °C with aeration at 220 r.p.m.. Bacteria were grown to an OD of 0.5, and then the cells concentration was adjusted to ≈1×10^6 cells per mL. Bacteria were then challenged with nisin (2*MIC), silver nitrate or Ag-nisin NP (2*MIC) in culture tubes at 37 °C and 220 r.p.m. Non-treated bacteria were used as negative control (Untreated). At desired time points, 200 µL aliquots were taken, centrifuged at 8000 *g* for 2 min and resuspended in 200 µL of MHB. Ten-fold serially diluted samples were plated on MHA plates. After incubated at 37 °C overnight, colonies were counted and c.f.u. per mL was calculated. Each experiment was performed in triplicate.

4.5. Antibiofilm assay

The strains (*A. baumannii* (LMG01041), *P. aeruginosa* (LMG 6395), *E. coli* (LMG8223), *K. pneumoniae* (LMG20218) and *S. aureus* (LMG15975, MRSA) were cultured for one day at 37 ℃ in 4 mL of tryptone soya broth (TSB, Oxoid). The cultures were diluted to at an OD_{600} of 0.01 in TSB, and 200 µL of the resulting bacterial suspension was aliquoted into the wells of a 96-well tissue culture-treated polystyrene plate (corning). After 24 h of growth at 37 ℃, the plates were washed thoroughly three times with PBS to remove unattached bacteria. Next, MHB containing 0, 0.5, 1 and 2 times MIC of nisin, silver nitrate or Ag-nisin NP was added to the wells. The plates were incubated at 37 ℃ under shaking at 60 r.p.m.. XTT assay was used to assess the cell metabolically viability at 4 h post exposure to the tested compounds. Briefly, after having removed the compounds, the plates were washed vigorously three times with PBS. After that, PBS with 0.2 % glucose (200 µL) containing 50 µL XTT (Cell Proliferation Kit XTT, AppliChem) was added to the wells and incubated at 37 ℃ for 2 h. The plates were then determined using a Varioskan™ LUX multimode microplate reader (Thermo Fisher Scientific) at 485 nm (reference 690 nm). Higher OD values correlated to higher numbers of viable pathogens in the biofilm. Each experiment was performed in triplicate.

4.6. Cell culture

Human skin fibroblasts (Hs 44.Fs, ATCC ® CRL7024™) and the human kidney epithelium cell line (HEK) were maintained in complete DMEM supplemented with 10 % (v/v) foetal bovine serum (FBS, Gibco), 100 U/mL penicillin (HyClone), and 100 μg/mL streptomycin (HyClone). For the maintenance medium (MM), the serum concentration was reduced to 2%. Cells were incubated at 37 °C with 5% CO_2 [49].

4.7. Mammalian cell metabolic activity assay

The effect of our materials to mammalian cell metabolic activity was evaluated on Hs 44.Fs and HEK cells by using the XTT (Cell Proliferation Kit XTT, AppliChem) assay. Briefly, cells in 96-well plates were exposed to different concentrations of materials in sextuplet. The test samples were suspended in MM (100 μL per well). After 24 h incubation, the XTT reagent was added to the cultures according to the manufacturer's instructions, and the plates were incubated at 37 °C for 2 h with 5% CO_2. Then, the absorbance values were measured by using a Varioskan™ LUX multimode microplate reader (Thermo Fisher Scientific) at 485 nm (reference 690 nm). The 50 % cell toxicity (CC_{50}) of peptides was calculated as previous studies descried [49,50].

4.8. Statistical analysis

The statistical significance of the data was assessed using a two-tailed student's *t*-test with GraphPad Prism software 7. Correlation analyses were evaluated by pearson r2, ns: $p > 0.05$, *$p < 0.05$, **$p < 0.01$, and ***$p < 0.001$.

CRediT authorship contribution statement

Xinghong Zhao: Conceptualization, Methodology, Investigation, Writing - original draft. **Oscar P. Kuipers:** Supervision, Writing - review & editing.

Declaration of Competing Interest

The authors report no declarations of interest.

Acknowledgments

X. Zhao was financed by the Chinese Scholarship Council (CSC) and the Netherlands Organization for Scientific Research (NWO), research program TTW (17241). We thank Dr. Gert N. Moll (Lanthio Pharma, Rozenburglaan 13 B, Groningen, 9727 DL, Netherlands) for critically reading and improving the manuscript.

Appendix A. Supplementary data

Supplementary material related to this article can be found, in the online version, at doi:https://doi.org/10.1016/j.colsurfb.2021.111965.

References

[1] H. Vaez, F. Beigi, Antibiotic susceptibility patterns of aerobic bacterial strains isolated from patients with burn wound infections, Germs 6 (2016) 34.
[2] R.R. Pallavali, V.L. Degati, D. Lomada, M.C. Reddy, V.R.P. Durbaka, Isolation and in vitro evaluation of bacteriophages against MDR-bacterial isolates from septic wound infections, PLoS One 12 (2017), e0179245.
[3] L.J. Bessa, P. Fazii, M. Di Giulio, L. Cellini, Bacterial isolates from infected wounds and their antibiotic susceptibility pattern: some remarks about wound infection, Int. Wound J. 12 (2015) 47–52.
[4] N.P. Singh, M. Rani, K. Gupta, T. Sagar, I.R. Kaur, Changing trends in antimicrobial susceptibility pattern of bacterial isolates in a burn unit, Burns 43 (2017) 1083–1087.
[5] B.M. Yasidi, D.B. Akawu, O.J. Oihoma, J.Y. Bara, U.H. Mohammed, G. N. Mohammed, Z.B. Ali, L. Joshua, H. Ibrahim, O.K. Okwong, Retrospective analysis of bacterial pathogens isolated from wound infections at a Tertiary Hospital in Nguru, Yobe State Nigeria, Am. J. Biomed. Life Sci. 3 (2015) 1–6.
[6] A.E. Barsoumian, K. Mende, C.J. Sanchez, M.L. Beckius, J.C. Wenke, C.K. Murray, K.S. Akers, Clinical infectious outcomes associated with biofilm-related bacterial infections: a retrospective chart review, BMC Infect. Dis. 15 (2015) 223.
[7] Y. Liu, L. Shi, L. Su, H.C. van der Mei, P.C. Jutte, Y. Ren, H.J. Busscher, Nanotechnology-based antimicrobials and delivery systems for biofilm-infection control, Chem. Soc. Rev. 48 (2019) 428–446.
[8] B. Le Ouay, F. Stellacci, Antibacterial activity of silver nanoparticles: a surface science insight, Nano Today 10 (2015) 339–354.
[9] A. Panáček, M. Smékalová, M. Kilianová, R. Prucek, K. Bogdanová, R. Večeřová, M. Kolář, M. Havrdová, G. Płaza, J. Chojniak, Strong and nonspecific synergistic antibacterial efficiency of antibiotics combined with silver nanoparticles at very low concentrations showing no cytotoxic effect, Molecules 21 (2016) 26.
[10] K. Jyoti, M. Baunthiyal, A. Singh, Characterization of silver nanoparticles synthesized using Urtica dioica Linn. leaves and their synergistic effects with antibiotics, J. Radiat. Res. Appl. Sci. 9 (2016) 217–227.
[11] A. Panáček, M. Smékalová, R. Večeřová, K. Bogdanová, M. Röderová, M. Kolář, M. Kilianová, Š. Hradilová, J.P. Froning, M. Havrdová, Silver nanoparticles strongly enhance and restore bactericidal activity of inactive antibiotics against multiresistant Enterobacteriaceae, Colloids Surf. B Biointerfaces 142 (2016) 392–399.
[12] J.R. Morones-Ramirez, J.A. Winkler, C.S. Spina, J.J. Collins, Silver enhances antibiotic activity against gram-negative bacteria, Sci. Transl. Med. 5 (2013) 190ra81.
[13] P.D. Cotter, C. Hill, R.P. Ross, Food microbiology: bacteriocins: developing innate immunity for food, Nat. Rev. Microbiol. 3 (2005) 777.
[14] L.J. de Arauz, A.F. Jozala, P.G. Mazzola, T.C.V. Penna, Nisin biotechnological production and application: a review, Trends Food Sci. Technol. 20 (2009) 146–154.
[15] H.E. Hasper, N.E. Kramer, J.L. Smith, J.D. Hillman, C. Zachariah, O.P. Kuipers, B. De Kruijff, E. Breukink, An alternative bactericidal mechanism of action for lantibiotic peptides that target lipid II, Science 313 (5793) (2006) 1636–1637.
[16] E. Breukink, B. de Kruijff, Lipid II as a target for antibiotics, Nat. Rev. Drug Discov. 5 (2006) 321.
[17] X. Zhao, Z. Yin, E. Breukink, G.N. Moll, O.P. Kuipers, An engineered double lipid II binding motifs-containing lantibiotic displays potent and selective antimicrobial activity against E. faecium, Antimicrob. Agents Chemother. 64 (6) (2020), e02050-19.
[18] R. Rink, J. Wierenga, A. Kuipers, L.D. Kluskens, A.J.M. Driessen, O.P. Kuipers, G. N. Moll, Dissection and modulation of the four distinct activities of nisin by mutagenesis of rings A and B and by C-terminal truncation, Appl. Environ. Microbiol. 73 (2007) 5809–5816.
[19] J.M. Shin, J.W. Gwak, P. Kamarajan, J.C. Fenno, A.H. Rickard, Y.L. Kapila, Biomedical applications of nisin, J. Appl. Microbiol. 120 (2016) 1449–1465.
[20] S.E. Murinda, K.A. Rashid, R.F. Roberts, In vitro assessment of the cytotoxicity of nisin, pediocin, and selected colicins on simian virus 40–transfected human colon and Vero monkey kidney cells with trypan blue staining viability assays, J. Food Prot. 66 (2003) 847–853.
[21] J.M. Shin, I. Ateia, J.R. Paulus, H. Liu, J.C. Fenno, A.H. Rickard, Y.L. Kapila, Antimicrobial nisin acts against saliva derived multi-species biofilms without cytotoxicity to human oral cells, Front. Microbiol. 6 (2015) 617.
[22] G. Singh, P.K. Babele, S.K. Shahi, R.P. Sinha, M.B. Tyagi, A. Kumar, Green synthesis of silver nanoparticles using cell extracts of Anabaena doliolum and screening of its antibacterial and antitumor activity, J. Microbiol. Biotechnol. 24 (2014) 1354–1367.
[23] J. Fei, J. Zhao, C. Du, A. Wang, H. Zhang, L. Dai, J. Li, One-pot ultrafast self-assembly of autofluorescent polyphenol-based core@ shell nanostructures and their selective antibacterial applications, ACS Nano 8 (2014) 8529–8536.
[24] M. Chopra, P. Kaur, M. Bernela, R. Thakur, Surfactant assisted nisin loaded chitosan-carageenan nanocapsule synthesis for controlling food pathogens, Food Control 37 (2014) 158–164.
[25] X. Qi, G. Poernomo, K. Wang, Y. Chen, M.B. Chan-Park, R. Xu, M.W. Chang, Covalent immobilization of nisin on multi-walled carbon nanotubes: superior antimicrobial and anti-biofilm properties, Nanoscale 3 (2011) 1874–1880.
[26] C. Wu, T. Wu, Z. Fang, J. Zheng, S. Xu, S. Chen, Y. Hu, X. Ye, Formation, characterization and release kinetics of chitosan/γ-PGA encapsulated nisin nanoparticles, RSC Adv. 6 (2016) 46686–46695.
[27] E.I. Alarcon, C.J. Bueno-Alejo, C.W. Noel, K.G. Stamplecoskie, N.L. Pacioni, H. Poblete, J.C. Scaiano, Human serum albumin as protecting agent of silver nanoparticles: role of the protein conformation and amine groups in the nanoparticle stabilization, J. Nanopart. Res. 15 (2013) 1–14.
[28] E.I. Alarcon, K. Udekwu, M. Skog, N.L. Pacioni, K.G. Stamplecoskie, M. González-Béjar, N. Polisetti, A. Wickham, A. Richter-Dahlfors, M. Griffith, The biocompatibility and antibacterial properties of collagen-stabilized, photochemically prepared silver nanoparticles, Biomaterials 33 (2012) 4947–4956.
[29] M. Vignoni, H. de Alwis Weerasekera, M.J. Simpson, J. Phopase, T.-F. Mah, M. Griffith, E.I. Alarcon, J.C. Scaiano, LL37 peptide@ silver nanoparticles: combining the best of the two worlds for skin infection control, Nanoscale 6 (2014) 5725–5728.
[30] S. Schmitt, M. Montalbán-López, D. Peterhoff, J. Deng, R. Wagner, M. Held, O. P. Kuipers, S. Panke, Analysis of modular bioengineered antimicrobial lanthipeptides at nanoliter scale, Nat. Chem. Biol. 15 (2019) 437.

[31] Q. Li, M. Montalban-Lopez, O.P. Kuipers, Increasing the antimicrobial activity of nisin-based lantibiotics against Gram-negative pathogens, Appl. Environ. Microbiol. 84 (2018) e00052–18.
[32] X. Zhao, O.P. Kuipers, Nisin-and ripcin-derived hybrid lanthipeptides display selective antimicrobial activity against Staphylococcus aureus, ACS Synth. Biol. (2021), https://doi.org/10.1021/acssynbio.1c00080.
[33] S.A. Cochrane, B. Findlay, A. Bakhtiary, J.Z. Acedo, E.M. Rodriguez-Lopez, P. Mercier, J.C. Vederas, Antimicrobial lipopeptide tridecaptin A1 selectively binds to Gram-negative lipid II, Proc. Natl. Acad. Sci. 113 (2016) 11561–11566.
[34] L.L. Ling, T. Schneider, A.J. Peoples, A.L. Spoering, I. Engels, B.P. Conlon, A. Mueller, T.F. Schäberle, D.E. Hughes, S. Epstein, A new antibiotic kills pathogens without detectable resistance, Nature 517 (2015) 455.
[35] R.K. Pettit, C.A. Weber, M.J. Kean, H. Hoffmann, G.R. Pettit, R. Tan, K.S. Franks, M.L. Horton, Microplate Alamar blue assay for Staphylococcus epidermidis biofilm susceptibility testing, Antimicrob. Agents Chemother. 49 (2005) 2612–2617.
[36] H.-J. Tang, C.-C. Chen, K.-C. Cheng, H.-S. Toh, B.-A. Su, S.-R. Chiang, W.-C. Ko, Y.-C. Chuang, In vitro efficacy of fosfomycin-containing regimens against methicillin-resistant Staphylococcus aureus in biofilms, J. Antimicrob. Chemother. 67 (2012) 944–950.
[37] J. Kwieciński, S. Eick, K. Wójcik, Effects of tea tree (Melaleuca alternifolia) oil on Staphylococcus aureus in biofilms and stationary growth phase, Int. J. Antimicrob. Agents 33 (2009) 343–347.
[38] Q.Q. Zhang, Y.H. Zhang, F.Y. Cai, X.L. Liu, X.H. Chen, M. Jiang, Comparative antibacterial and antibiofilm activities of garlic extracts, nisin, ε-polylysine, and citric acid on Bacillus subtilis, J. Food Process. Preserv. 43 (2019), e14179.
[39] R. Kajwadkar, J.M. Shin, G.-H. Lin, J.C. Fenno, A.H. Rickard, Y.L. Kapila, High-purity nisin alone or in combination with sodium hypochlorite is effective against planktonic and biofilm populations of Enterococcus faecalis, J. Endod. 43 (2017) 989–994.
[40] S. Iravani, H. Korbekandi, S.V. Mirmohammadi, B. Zolfaghari, Synthesis of silver nanoparticles: chemical, physical and biological methods, Res. Pharm. Sci. 9 (2014) 385.
[41] V. Polshettiwar, M.N. Nadagouda, R.S. Varma, Microwave-assisted chemistry: a rapid and sustainable route to synthesis of organics and nanomaterials, Aust. J. Chem. 62 (2009) 16–26.
[42] M.N. Nadagouda, T.F. Speth, R.S. Varma, Microwave-assisted green synthesis of silver nanostructures, Acc. Chem. Res. 44 (2011) 469–478.
[43] M. Moein, A.A.I. Fooladi, H.M. Hosseini, Determining the effects of green chemistry synthesized Ag-nisin nanoparticle on macrophage cells, Microb. Pathog. 114 (2018) 414–419.
[44] I. Chopra, The increasing use of silver-based products as antimicrobial agents: a useful development or a cause for concern? J. Antimicrob. Chemother. 59 (2007) 587–590.
[45] A. Besinis, T. De Peralta, R.D. Handy, Inhibition of biofilm formation and antibacterial properties of a silver nano-coating on human dentine, Nanotoxicology 8 (2014) 745–754.
[46] H. Qin, H. Cao, Y. Zhao, C. Zhu, T. Cheng, Q. Wang, X. Peng, M. Cheng, J. Wang, G. Jin, In vitro and in vivo anti-biofilm effects of silver nanoparticles immobilized on titanium, Biomaterials 35 (2014) 9114–9125.
[47] K. Markowska, A.M. Grudniak, K.I. Wolska, Silver nanoparticles as an alternative strategy against bacterial biofilms, Acta Biochim. Pol. 60 (2013).
[48] I. Wiegand, K. Hilpert, R.E.W. Hancock, Agar and broth dilution methods to determine the minimal inhibitory concentration (MIC) of antimicrobial substances, Nat. Protoc. 3 (2008) 163.
[49] X. Zhao, Q. Cui, Q. Fu, X. Song, R. Jia, Y. Yang, Y. Zou, L. Li, C. He, X. Liang, L. Yin, J. Lin, G. Ye, G. Shu, L. Zhao, F. Shi, C. Lv, Z. Yin, Antiviral properties of resveratrol against pseudorabies virus are associated with the inhibition of IκB kinase activation, Sci. Rep. 7 (1) (2017) 1–11, https://doi.org/10.1038/s41598-017-09365-0.
[50] L.J. Reed, H. Muench, A simple method of estimating fifty per cent endpoints, Am. J. Epidemiol. 27 (1938).